RIDING COMFORT OF A DOUBLE-DECK LONG-SPAN BRIDGE UNDER BOTH ROAD VEHICLES AND MONORAIL TRAINS

X.T. Si [1], Francis T.K. Au [1] and W.H. Guo[2]
[1] Department of Civil Engineering,
The University of Hong Kong, Hong Kong, China
[2] School of Civil Engineering and Architecture,
Central South University, Changsha, Hunan, China

ABSTRACT

This paper presents a method for three-dimensional dynamic analysis of double-deck long-span bridges carrying road vehicles and monorail trains considering the effects of vertical and horizontal surface roughness of the bridge deck and rail tracks respectively. The road vehicle is modelled as a mass-spring-damper system with 7 degrees of freedom (DOFs) while that of the monorail train has 15 DOFs. Then a fully computerized approach is adopted to assemble the governing equation of motion of the coupled system. This coupled system can be reduced to a vehicle-bridge or train-bridge interaction system. Based on this framework, dynamic analysis of a long-span bridge carrying both road vehicles and monorail trains is carried out to investigate the effects of vehicles on the riding comfort of monorail trains and vice versa.

KEYWORDS

Bridge-vehicle interaction, long-span bridges, monorail trains, road vehicles, surface roughness.

INTRODUCTION

Heavy road vehicles and railway trains running on a long-span bridge may significantly change the overall dynamic behaviour and affect the fatigue life of local members. The vibrating bridge will in turn affect the safety and riding comfort of the road vehicles and trains moving on it. Therefore, the dynamic interaction between road vehicles, trains and long-span bridges becomes an important problem which attracts the attention of many researchers.

Kim et al. (2005) proposed a spatial method of analysis for bridge-vehicle interaction of a steel girder bridge and vehicles, in which governing equations of motion for the coupled system were derived using Lagrange equation taking account of roadway roughness. Another method was developed by Cai and Chen (2004) for analysis of coupled three-dimensional vehicle-bridge systems under strong winds. Guo and Xu (2001, 2002, 2000) and Xu and Guo (2000) also developed a fully computerized approach to study the dynamic response of cable-stayed bridges under moving heavy vehicles and estimated the riding comfort of vehicles on bridges under crosswind. As for coupled train-bridge systems, Au et al. (2001, 2002) investigated the impact of cable-stayed bridges under moving railway traffic in which a train was idealized as a four-axle system with 10 degrees-of- freedom (DOFs). Yau et al. (1999) studied the impact response of high speed rail bridge and assessed the riding comfort of railcars. It was found that the rail irregularity, ballast stiffness, suspension damping could drastically affect the riding comfort of rail cars travelling over simple beams. To investigate the riding comfort of monorail trains on bridges, Lee et al. (2006, 2005) introduced a procedure for analysis of train-bridge interaction by using Lagrange formulation for monorail trains and finite element method for modal analysis of monorail bridges. The dynamic responses of a steel monorail bridge under a moving train were studied using the above procedure, but it only focused on the dynamic responses of short-span simply supported bridges under moving trains.

The above review shows that most of the previous research studies have focused on bridges carrying either road vehicles or rail trains but not both at the same time. So far not much comprehensive analysis of bridges carrying both road vehicles and rail trains has been done. This paper describes a framework developed for dynamic analysis of a three-dimensional coupled system comprising a long-span bridge carrying road vehicles and monorail trains travelling at different speeds taking into account the effects of surface roughness.

IDEALIZATION OF THE COUPLED SYSTEM

Idealization of the Bridge

After setting the global coordinate system comprising *X*-, *Y*-, and *Z*- axes respectively in the longitudinal, lateral and vertical directions of the bridges following the right-handed rule, a bridge can be modelled by finite element method using spatial beam elements, cable elements, truss elements, etc for dynamic analysis. Consistent mass matrices and Rayleigh damping are used to build up the bridge model. Finally, the motion equation of a bridge is obtained as:

$$[M_b]\{\ddot{v}_b\}+[C_b]\{\dot{v}_b\}+[K_b]\{v_b\}=\{P_{be}\} \tag{1}$$

where$[M_b]$, $[C_b]$, and $[K_b]$ denote the mass, damping and stiffness matrices of the bridge respectively. $\{\ddot{v}_b\}$, $\{\dot{v}_b\}$ and $\{v\}$ are nodal dynamic acceleration, velocity and displacement vectors of the bridge correspondingly and $\{P_{be}\}$ is the external force vector of the bridge.

Idealization of a Road Vehicle

A road vehicle can be modeled as a mass-spring-damper system. Figure 2 shows a spatial model of a heavy road vehicle with 7 DOFs composed of a car body with motion of bouncing Z_{vc}, pitching θ_{vc} and rolling ϕ_{vc} and four tires with only motion of bouncing Z_{vt}. The parameters *K, M* and *C* denote spring constant, mass and damping coefficient respectively. Subscript *vc* denotes the car body of the vehicle; *i* indicates the lane number where the vehicle runs; *j* indicates the number of the vehicle in a vehicular motorcade.

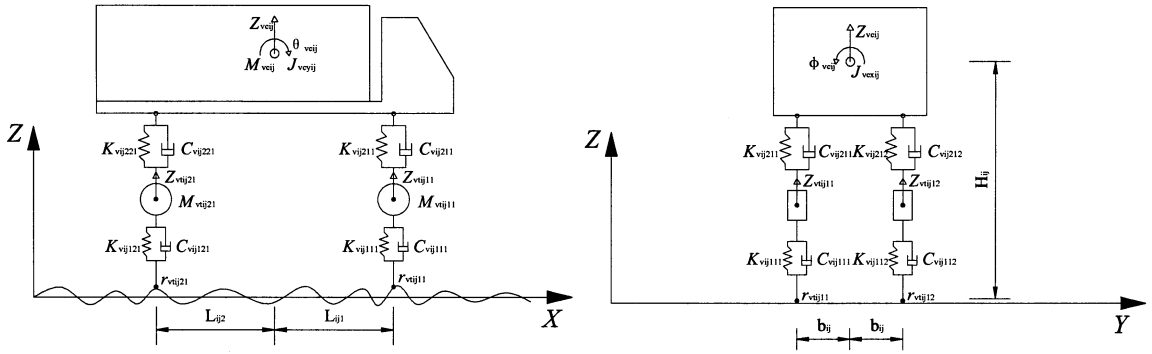

Figure 1 An idealized spatial model of a heavy road vehicle with 7 DOFs

The assumptions made in this study are: (1) the vehicle speed and path are constant; (2) the suspension springs are linearly elastic and the damping of the suspension system is viscous and (3) the bridge deck and the tires of the vehicles are in good contact without separation.

The relative spring deformation of air suspension can be expressed as follows:

$$R_{vij2kl}=Z_{vcij}+(-1)^k L_{ijk}\theta_{vcij}+(-1)^l b_{ij}\phi_{vcij}-Z_{vtijkl} \tag{2}$$

While the relative spring deformation at each tire can be obtained by:

$$R_{vij1kl}=Z_{vtijkl}-V_{btijkl}-r_{btijkl} \tag{3}$$

where r_{btijkl} is the bridge deck roughness at the contact point. Subscripts *vc* and *vt* denote the car body and vehicular tires respectively; *k* is the axle index (*k*=1, 2 for the front and rear axle respectively); *l* indicates the tire position in an axle (*l*=1,2 for the left and right positions of an axle respectively); V_{btijkl} denotes the vertical displacement of the bridge at the contact point. The vertical displacement V_{btijkl} is given by

$$V_{btijkl}=[N_1\ N_2\ (e_{btijkl}N_5)\ N_3\ N_4\ (e_{btijkl}N_6)]_{x=x_e}[Z^{ei}\ \theta^{ei}\ \phi^{ei}\ Z^{ej}\ \theta^{ej}\ \phi^{ej}]^T \tag{4}$$

where N_1, N_2, N_3, N_4, N_5 and N_6 are the shape functions of the spatial beam element; Z^{ei}, θ^{ei} and ϕ^{ei} are, respectively, the vertical displacement and rotations about *Y*- and *X*- axes of Node *i* of the corresponding beam element, while Z^{ej}, θ^{ej} and ϕ^{ej} are those of Node *j* of the element; and *e* is the horizontal distance between the contact point and center of the corresponding bridge element.

The deformation rates of the spring can be obtained by differentiation of the relative deformation:

$$\dot{R}_{vij2kl} = \dot{Z}_{vcij} + (-1)^k L_{ijk}\dot{\theta}_{vcij} + (-1)^l b_{ij}\dot{\phi}_{vcij} - \dot{Z}_{vtijkl} \tag{5}$$

$$\dot{R}_{vij1kl} = \dot{Z}_{vtijkl} - N_1(x_c)\dot{Z}^{ei}_{btijkl} - N_2(x_c)\dot{\theta}^{ei}_{btijkl} - e_{btijkl}N_5(x_c)\phi^{ei}_{btijkl}$$

$$- N_3(x_c)\dot{Z}^{ej}_{btijkl} - N_4(x_c)\dot{\theta}^{ej}_{btijkl} - e_{btijkl}N_6(x_c)\phi^{ej}_{btijkl} - \frac{\partial r_{btijkl}(x)}{\partial x}U_{vij} \tag{6}$$

where U_v is the speed of vehicle and the dot denotes differentiation with respect to time t.

Idealization of Monorail Train

A monorail train (Figure 2(d)) has two bogies each of which has a front axle and a rear axle. Each bogie has pneumatic tires for travelling and steeling as well as stabilizing wheels that firmly grasp the track girder.

Figure 2(a), 2(b) and 2(c) show an idealized railcar model with 15 DOFs. A coordinate system similar to that of the bridge is adopted. Bouncing, swaying, pitching, rolling and yawing motion of the body and each bogie are incorporated into the model. The track and wheel are assumed to be in a good contact and there is no concentrated mass at each contact point.

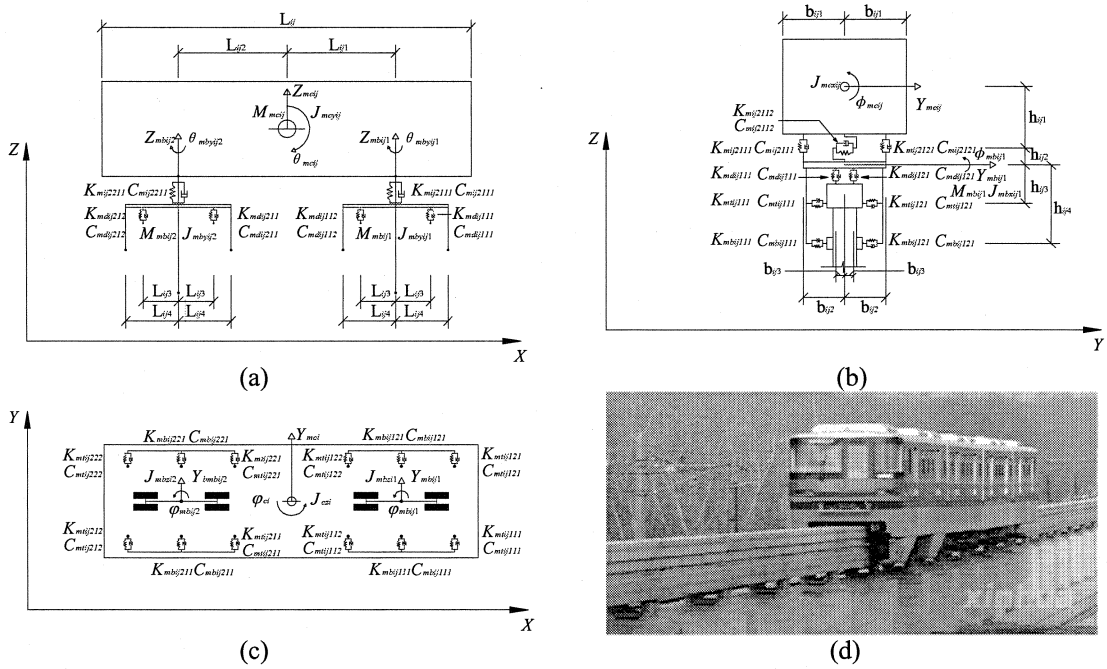

Figure 2 Idealized model of a monorail car with 15 DOFs

The vertical and lateral relative spring deformations of air suspension can be calculated respectively as follows:

$$R_{mij2kl1} = Z_{mcij} + (-1)^k \theta_{mcij}L_{ijk} + (-1)^l \phi_{mcij}b_{ij1} - Z_{mbijk} - (-1)^l \phi_{mbijk}b_{ij2} \tag{7}$$

$$R_{mij2k12} = Y_{mcij} - (-1)^k \varphi_{mcij}L_{ijk} + \phi_{mcij}h_{ij1} - Y_{mbijk} + \phi_{mbijk}h_{ij2} \tag{8}$$

The relative spring deformation at the driving, steering and stabilizing wheel can be obtained respectively as follows:

$$R_{mdijklp} = Z_{mbijk} + (-1)^p \theta_{mbijk}L_{ij3} + (-1)^l \phi_{mbijk}b_{ij3} - V_{bdijklp} - r_{bdijklp} \tag{9}$$

$$R_{mtijklp} = Y_{mbijk} - (-1)^p \varphi_{mbijk}L_{ij4} + \phi_{mbijk}h_{ij3} - V_{btijklp} - r_{mtijklp} \tag{10}$$

$$R_{mbijklp} = Y_{mbijk} + \varphi_{mbijk}h_{ij4} - V_{bbijklp} - r_{mbijklp} \tag{11}$$

Where $V_{bdijklp}$, $V_{btijklp}$ and $V_{bbijklp}$ denote the displacement of the bridge at the contact point respectively; $r_{bdijklp}$, $r_{btijklp}$ and $r_{bbijklp}$ denote the surface roughness values at the contact points of driving, steering and stabilizing wheels; subscripts *md*, *mt* and *mb* denote the driving, steering and stabilizing wheels; *i* is the lane number where the monorail trains run; *j* is the serial number of the train in the motorcade; *k* denote the position of the bogie; *p* denotes the wheel position in a bogie (p=1,2 for the front and rear sides respectively); and index *l* denotes the wheel position in an axle (l=1,2 for the left and right sides respectively).

The displacements of the bridge at the contact points can be calculated as follows:

$$V_{bdijklp} = [N_1\ N_2\ (e_{bdijklp}N_5)\ N_3\ N_4\ (e_{bdijklp}N_6)]_{x=x_c}[Z^{ei}\ \theta^{ei}\ \phi^{ei}\ Z^{ej}\ \theta^{ej}\ \phi^{ej}]^T_{bdijklp} \tag{12}$$

$$V_{btijklp} = [N_1\ N_2\ (h_{btijklp}N_5)\ N_3\ N_4\ (e_{btijklp}N_6)]_{x=x_c}[Y^{ei}\ \varphi^{ei}\ \phi^{ei}\ Y^{ej}\ \varphi^{ej}\ \phi^{ej}]^T_{btijklp} \tag{13}$$

$$V_{bbijklp} = [N_1\ N_2\ (h_{bbijklp}N_5)\ N_3\ N_4\ (e_{bbijklp}N_6)]_{x=x_c}[Y^{ei}\ \varphi^{ei}\ \phi^{ei}\ Y^{ej}\ \varphi^{ej}\ \phi^{ej}]^T_{bbijklp} \tag{14}$$

where e and h are the horizontal and vertical distances between the contact point and center of the corresponding bridge element respectively.

The deformation rate of each spring can be obtained by differentiation of the relative deformation:

$$\dot{R}_{mij2kl1} = \dot{Z}_{mcij} + (-1)^k \dot{\theta}_{mcij}L_{ijk} + (-1)^l \dot{\phi}_{mcij}b_{ij1} - \dot{Z}_{mbijk} - (-1)^l \dot{\phi}_{mbijk}b_{ij2} \tag{15}$$

$$\dot{R}_{mij2k12} = \dot{Y}_{mcij} - (-1)^k \dot{\varphi}_{mcij}L_{ijk} + \dot{\phi}_{mcij}h_{ij1} - \dot{Y}_{mbijk} + \dot{\phi}_{mbijk}h_{ij2} \tag{16}$$

$$\begin{aligned}\dot{R}_{mdijklp} &= \dot{Z}_{mbijk} + (-1)^p \dot{\theta}_{mbijk}L_{ij3} + (-1)^l \dot{\phi}_{mbijk}b_{ij3} - N_1(x_c)\dot{Z}^{ei}_{bdijklp} - N_4(x_c)\dot{\theta}^{ej}_{bdijklp} \\ &- e_{bdijklp}N_5(x_c)\dot{\phi}^{ei}_{bdijklp} - e_{bdijklp}N_6(x_c)\dot{\phi}^{ej}_{bdijklp} - N_2(x_c)\dot{\theta}^{ei}_{bdijklp} - N_3(x_c)\dot{Z}^{ej}_{bdijklp} - \frac{\partial r_{bdijklp}(x)}{\partial x}U_{mij}\end{aligned} \tag{17}$$

$$\begin{aligned}\dot{R}_{mtijklp} &= \dot{Y}_{mbijk} + (-1)^p \dot{\varphi}_{mbijk}L_{ij4} + \dot{\phi}_{mbijk}h_{ij3} - N_1(x_c)\dot{Y}^{ei}_{btijklp} - N_2(x_c)\dot{\varphi}^{ei}_{btijklp} \\ &- h_{btijklp}N_5(x_c)\dot{\phi}^{ei}_{btijklp} - h_{btijklp}N_6(x_c)\dot{\phi}^{ej}_{btijklp} - N_4(x_c)\dot{\varphi}^{ej}_{btijklp} - N_3(x_c)\dot{Y}^{ej}_{btijklp} - \frac{\partial r_{btijklp}(x)}{\partial x}U_{mij}\end{aligned} \tag{18}$$

$$\begin{aligned}\dot{R}_{mbijklp} &= \dot{Y}_{mbijk} + \dot{\phi}_{mbijk}h_{ij4} - N_1(x_c)\dot{Y}^{ei}_{bbijklp} - N^*_2(x_c)\dot{\varphi}^{ei}_{bbijklp} \\ &- h_{bbijklp}N_5(x_c)\dot{\phi}^{ei}_{bbijklp} - h_{bbijklp}N_6(x_c)\dot{\phi}^{ej}_{bbijklp} - N^*_4(x_c)\dot{\varphi}^{ej}_{bbijklp} - N_3(x_c)\dot{Y}^{ej}_{bbijklp} - \frac{\partial r_{bbijklp}(x)}{\partial x}U_{mij}\end{aligned} \tag{19}$$

where U_m is the speed of monorail trains.

Modelling of Bridge Deck and Track Irregularities

The surface roughness of a bridge is one of the important factors to excite a vehicle-bridge system (Yau et al., 1999, Au et al., 2002, Cai and Chen, 2004). It can be taken to be a zero-mean stationary Gaussian random process and simulated with the method of spectral representation based on a specified power spectral density (PSD) (Guo and Xu, 2001):

$$S_v(\bar{\phi}) = A_r(\frac{\bar{\phi}}{\bar{\phi}_0})^{-2} \tag{20}$$

where $\bar{\phi}$ is the spatial frequency; $\bar{\phi}_0$ ($=1/2\pi$) is a non-continuous frequency coefficient, A_r is the surface roughness coefficient of bridge deck.

The PSD function adopted for the rail surface roughness is (Lee et al., 2006, Lee et al., 2005):

$$S_{z0}(\Omega) = \frac{\alpha}{\Omega^n + \beta^n} \tag{21}$$

where Ω ($=\omega/2\pi$) is the spatial frequency; α , β and n are the roughness coefficient, shape parameter and a parameter to express the power distribution of a given PSD curve respectively. The surface roughness is simulated by the spectral representation method based on:

$$r(x) = \sum_{k=1}^{N}\sqrt{2S(\bar{\Omega}_k)\Delta\bar{\Omega}}\cos(2\pi\Delta\bar{\Omega}_k x + \theta_k) \tag{22}$$

Where θ_k is a random phase angle complying with a uniform distribution from 0 to 2π .

The Coupled System Comprising Bridge, Road Vehilces and Monorail Trains

Assuming that all relevant displacements remain small, the principle of virtual work can be used to derive the governing equation of the coupled train-bridge system. The equilibrium condition of the bridge under its self-weight without any vehicle is taken as the initial condition. Then the virtual work δW done by inertial forces, damping forces, elastic forces and external loading can be obtained, thereby giving:

$$\delta W^v_I + \delta W^m_I + \delta W^b_I + \delta W^v_D + \delta W^m_D + \delta W^b_D + \delta W^v_S + \delta W^m_S + \delta W^b_S + \delta W^b_{Ex} = 0 \tag{23}$$

where the subscript *I, D, S* and *Ex* stand for inertial, damping, elastic and external effects respectively; and the subscripts *v, m* and *b* denote the vehicle, monorail train and bridge respectively. Finally the governing equation of the coupled system can be written as:

$$[M_{bmv}]\{\ddot{v}_{bmv}\}+[C_{bmv}]\{\dot{v}_{bmv}\}+[K_{bmv}]\{v_{bmv}\}=\{P_{bmv}\} \tag{24}$$

in which

$$\{v_{bmv}\}=\begin{Bmatrix} v_b \\ v_m \\ v_v \end{Bmatrix},\ [M_{bmv}]=\begin{bmatrix} M_b+M_{bbm}+M_{bbv} & 0 & 0 \\ 0 & M_m & 0 \\ 0 & 0 & M_v \end{bmatrix},\ [C_{bmv}]=\begin{bmatrix} C_b+C_{bbm1}+C_{bbv1} & C_{bm1} & C_{bv1} \\ C_{mb1} & C_m+C_{m1} & 0 \\ C_{vb1} & 0 & C_v+C_{v1} \end{bmatrix}$$

$$[K_{bmv}]=\begin{bmatrix} K_b+K_{bbm1}+K_{bbv1} & K_{bm1} & K_{bv1} \\ K_{mb1} & K_m+K_{m1} & 0 \\ K_{vb1} & 0 & K_v+K_{v1} \end{bmatrix},\ \{P_{bmv}\}=\begin{Bmatrix} \begin{bmatrix} P_{bmg}+P_{bmr1}+P_{bmr2}+P_{bmr3} \\ +P_{vbg}+P_{bvr1}+P_{bvr2}++P_{bvr3} \end{bmatrix} \\ P_{mr2}+P_{mr3} \\ P_{vr2}+P_{vr3} \end{Bmatrix}$$

where $[M_{bmv}]$, $[C_{bmv}]$ and $[K_{bmv}]$ are the mass, damping and stiffness matrices of the coupled system respectively; $\{v_b\}$, $\{v_m\}$ and $\{v_v\}$ are the displacement vectors of the bridge, monorail trains and road vehicles respectively; $[M_b]$, $[C_b]$ and $[K_b]$ are the mass, damping and stiffness matrices of the bridge respectively; $[K_m]$ and $[C_m]$ are the stiffness and damping matrices of the monorail trains respectively; $[K_v]$ and $[C_v]$ are the stiffness and damping matrices of road vehicles respectively; $[M_{bbm}]$ and $[M_{bbv}]$ account for the inertia forces of masses, respectively, of monorail trains and vehicles at contact points due to the bridge accelerations; $[C_{bm1}]$ and $[C_{mb1}]$ account for the damping of suspension systems of monorail trains while $[C_{bv1}]$ and $[C_{vb1}]$ account for those of vehicles; $[K_{bm1}]$, $[K_{mb1}]$, $[K_{bv1}]$ and $[K_{vb1}]$ account for the corresponding stiffness of the suspension systems; $[C_{bbm1}]$ and $[C_{bbv1}]$ account for the additional effects on the bridge damping $[C_b]$ due to suspension systems of monorail trains and vehicles respectively; $[K_{bbm1}]$ and $[K_{bbv1}]$ account for the corresponding additional effects on the bridge stiffness $[K_b]$; $[C_{m1}]$ and $[C_{v1}]$ account for the additional effects of suspension on damping of monorail trains and road vehicles respectively; $[K_{m1}]$ and $[K_{v1}]$ account for the corresponding additional stiffness effects; $[P_{bmg}]$ and $[P_{bvg}]$ denote the loading from monorail trains and vehicles on the bridge; $[P_{bmr1}]$ and $[P_{bvr1}]$ account for the inertia forces of masses, respectively, of monorail trains and vehicles due to road roughness at contact points; $[P_{bmr2}]$, $[P_{bvr2}]$, $[P_{bmr3}]$ and $[P_{bvr3}]$ are additional force vectors acting on the bridge caused by the interaction between suspension and surface roughness; $[P_{mr2}]$ and $[P_{vr2}]$ account for the loading on monorail trains and vehicles respectively due to their damping at contact points and surface roughness; and $[P_{mr3}]$ and $[P_{vr3}]$ are force vectors acting on monorail trains and vehicles respectively due to their springs at contact points and surface roughness.

NUMERICAL STUDY

A computer program BRAVIN has been developed based on the proposed framework. The dynamic responses of a real long-span bridge carrying monorail trains and / or heavy road vehicles are investigated using the above program.

Prototype Bridge

Chongqing Caiyuanba Yangtze River Bridge is a steel tied-arch bridge carrying both road vehicles and monorail trains. The systematical double-deck bridge has an overall length of 800m with a main span of 420m and two side spans of 102m and 88m on each side (See Figure 3). Road vehicles run on the upper deck while monorail trains run on the track girders at the bottom chord of the truss. Figure 3 also shows locations A, B and C where more results will be worked out.

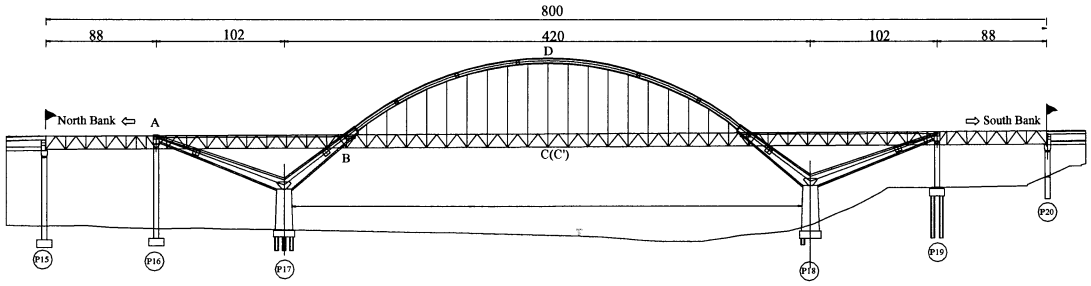

Figure 3 Chongqing Caiyuanba Bridge

A three-dimensional finite element model is established. The arch ribs and bracings between arch ribs are modelled by spatial beam elements, while the suspenders are modelled by spatial truss element. Spatial beam elements are also adopted for the steel truss, main piers, Y-shape rigid frames, etc. The connections between the bridge components and supports are also properly modelled.

Simulation of Surface Roughness of Bridge Deck and Monorail Track

The surface roughness of the bridge deck and monorail track girder is simulated by spectral representation. The roughness coefficient A_r in Eq.(20) is taken as 20×10^{-6} m^3/cycle according to International Organization for Standardization (ISO) specification for good roads (Guo, 2003). The simulation frequency range spans from 0.05Hz to 2Hz. The surface profiles of tracks for driving, steering and stabilizing wheels are simulated using parameters (Lee et al., 2006, Lee et al., 2005): (a) driving: α=0.0005, β=0.35, n=3.00; (b) steering: α=0.0006, β=0.5, n=2.80 and (c) stabilizing: α=0.0006, β=0.5, n=2.60 and a simulation frequency range from 0.01Hz to 2Hz. The simulated surface profiles for the bridge deck and monorail track respectively are shown in Figure 4 with a sample length of 3000m.

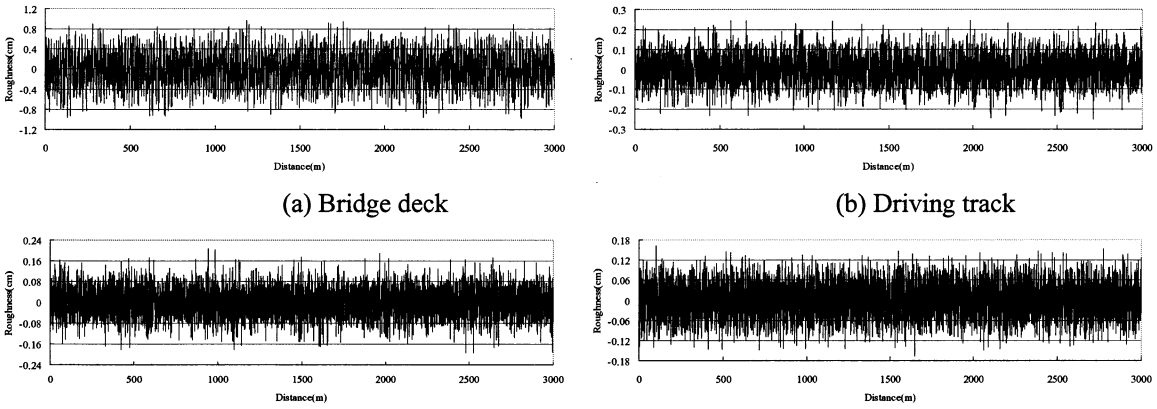

(a) Bridge deck (b) Driving track

(c) Stabilizing track (d) Steering track

Figure 4 Surface roughness of monorail track

Dynamic Responses of the Coupled System under Both Monorail Trains and Road Vehicles

Because of page limitation, only three cases are presented, namely: (1) Case SC: a motorcade of 20 heavy road vehicles at center to center spacing of 21m runs on Lane 2 (Figure 5(a)); (2) Case SM: a monorail train with 8 railcars at center to center spacing of 15.6m runs on the left track (Figure 5(b)); and (3) Case SMSC: both the motorcade in Case SC and the monorail train in Case SM run simultaneously. The speed is taken as 75km/h.

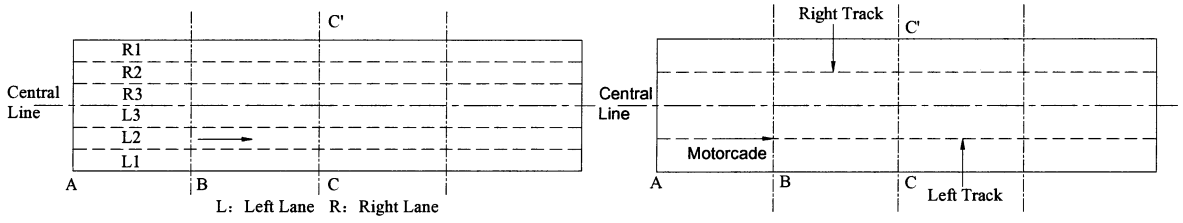

(a) (b)

Figure 5 Live load on the bridge: (a) road vehicles (b) monorail trains

The variations of vertical and lateral displacements at the middle of main span (Point C) are shown in Figure 8.

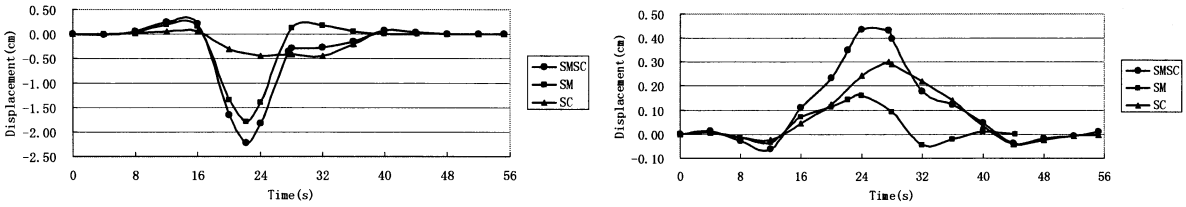

(a) Vertical (b) Lateral

Figure 6 Displacements of point C at the middle of main span

Figure 6 confirms that the dynamic responses of the bridge under both moving monorail trains and road vehicles are bigger than those under either monorail trains or road vehicles. The dynamic responses of the bridge are also significantly influenced by the monorail trains when both types of traffic run on the bridge simultaneously.

Riding Comfort of Monorail Trains and Road Vehicles

After obtaining the dynamic responses of the bridge, the riding comfort in terms of acceleration of the locomotive in the monorail train and the first road vehicle in the motorcade of all three cases is studied according to the relevant ISO Specifications. The results are shown in Figure 10 to Figure 12.

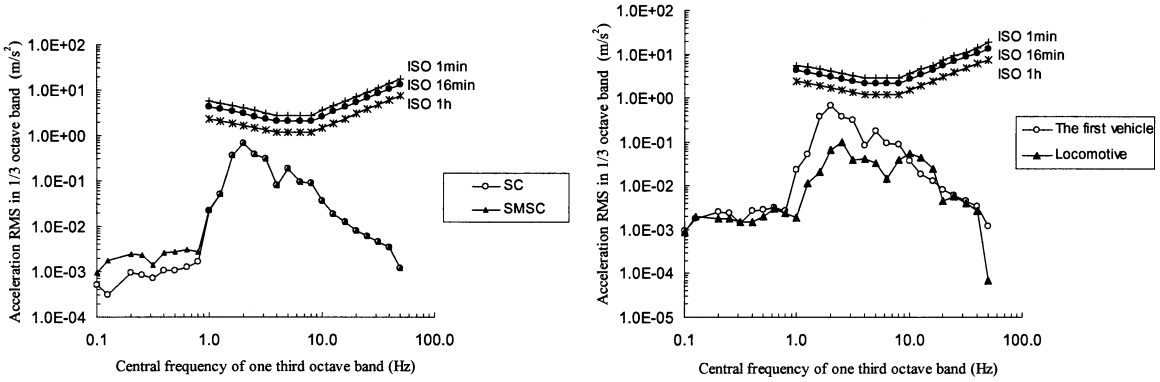

(a) (b)

Figure 7 Riding comfort in the vertical direction of: (a) the first vehicle of Cases SC and SMSC; (b) first road vehicle and locomotive of Case SMSC

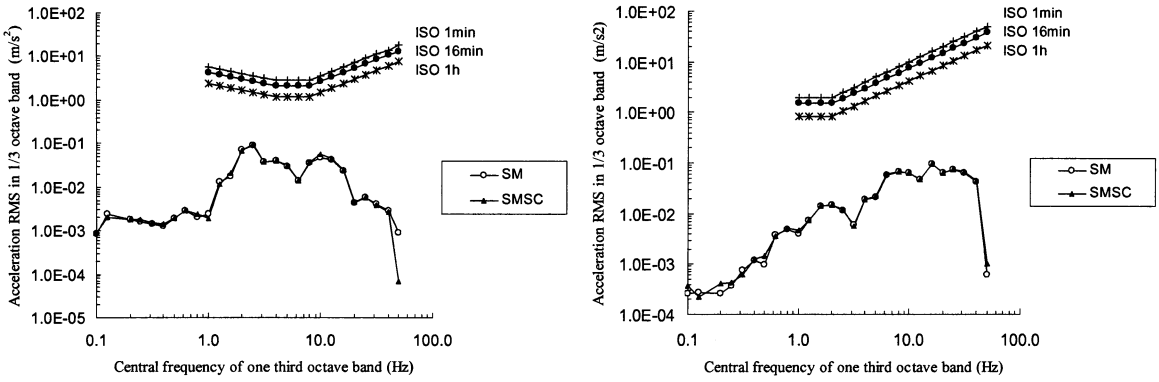

(a) Vertical (b) Lateral

Figure 8 Riding comfort of the locomotive of Cases SM and SMSC

Figure 7 and Figure 8 show that the root mean square accelerations in the one-third octave band of both the locomotive and the first vehicle in all calculated cases are lower than the allowable values, which indicates that their riding comfort can be classified as good.

Figure 7(a) shows that, when monorail trains move on the bridge, the riding comfort of the first road vehicle is reduced in the range of lower frequencies without affecting much in the range of higher frequencies. However,

Figure 10 shows that, compared with Case SM, the vehicle motorcade has no obvious effect on the riding comfort of the locomotive when they run on the bridge simultaneously.

Figure 7(b) indicates that passengers feel more comfortable in the monorail trains than in the heavy road vehicles in Case SMSC when both run simultaneously.

CONCLUSIONS

An analytical framework for the dynamic analysis of double-deck long-span bridges carrying road vehicles and / or monorail trains has been developed. It covers the modelling of road vehicles and monorail trains, as well as the bridge taking into account the vertical and lateral irregularities of monorail track and random roughness of bridge deck. The coupled system can be reduced to a vehicle-bridge or train-bridge interaction system easily. The case study of the Chongqing Caiyuanba Yangtze River Bridge carrying road vehicles and monorail trains demonstrates that the proposed framework can predict the dynamic behaviour of double-deck bridges under both road and railway traffic.

It is found that the monorail trains have more effect on the dynamic performance of the long-span bridge than road vehicles. The monorail trains can reduce the riding comfort of road vehicles in the range of lower frequencies compared with the case of road vehicles only. Therefore the effects in respect of riding comfort of trains on vehicles and vice versa should be considered carefully when designing a long-span bridge carrying both types of traffic.

ACKNOWLEDGMENTS

The authors gratefully acknowledge the financial support provided by the National Natural Science Foundation of China (Project No. 50208019) and the Research Grants Council (RGC) of the Hong Kong Special Administrative Region, China (RGC Project No. HKU 710208E).

REFERENCES

Au, F.T.K., Cheng, Y.S. and Cheung, Y.K. (2001). "Effect of random road roughness and long-term deflection of prestressed concrete girder and cable-stayed bridges on impact due to moving vehicles". *Computers and Structures,* 79, 853-872.

Au, F.T.K., Wang, J.J. and Cheung, Y.K. (2002). "Impact study of cable-stayed railway bridges with random rail irregularities". *Engineering Structures,* 24, 529-541.

Cai, C.S. and Chen, S.R. (2004). "Framework of vehicle-bridge-wind dynamic analysis". *Journal of Wind Engineering and Industrial Aerodynamics,* 92, 579-607.

Guo, W.H. (2003). "Dynamic analysis of coupled road vehicle and long span cable-stayed bridge systems under cross winds". Hong Kong, The Hong Kong Polytechnic University.

Guo, W.H. and Xu, Y.L. (2000). "Direct assembling matrix method for dynamic analysis of coupled vehicle-bridge system". *Proceedings of International Conference on Advances in Structural Dynamics.* Hong Kong.

Guo, W.H. and Xu, Y.L. (2001). "Fully computerized approach to study cable-stayed bridge-vehicle interaction". *Journal of Sound and Vibration,* 248, 745-761.

Guo, W.H. and Xu, Y.L. (2002). "Evaluation of ride comfort of road vehicles running on a cable-stayed bridge under crosswind". *Proceeding of the Third International Conference on Advances in Steel Structures.* Hong Kong.

Kim, C.W., Kawatani, M. and Kim, K.B. (2005). "Three-dimension dynamic analysis for bridge-vehicle interaction with roadway roughness". *Computers and Structures,* 83, 1627-1645.

Lee, C.H., Kawatani, M., Kim, C.W., Nishimura, N. and Kobayashi, Y. (2006). "Dynamic response of a monorail steel bridge under a moving train". *Journal of Sound and Vibration,* 294, 562-579.

Lee, C.H., Kim, C.W., Kawatani, M., Nishimura, N. and Kamizono, T. (2005). "Dynamic response analysis of monorail bridges under moving trains and riding comfort of trains". *Engineering Structures,* 27, 1999-2013.

Xu, Y.L. and Guo, W.H. (2000). "Dynamic analysis of cable-stayed bridge under a group of moving heavy vehicles". *International Symposium on Modern Concrete Composites & Infrastructures.* Beijing, China.

Yau, J.D., Yang, Y.B. and Kuo, S.R. (1999). "Impact response of high speed rail bridges and riding comfort of rail cars". *Engineering Structures,* 21, 836-844.